Contribution from the Structural Chemistry Group, Department of Chemistry, Indian Institute of Technology, Madras 600036, India

EPR and Electronic Structural Investigations of a Few Low-Spin Bis(tertiary phosphine) Complexes of Cobalt(II)

C. N. SETHULAKSHMI and P. T. MANOHARAN*

Received September 9, 1980

Preparation and electronic structural investigations of some low-spin Co(II) complexes of the ligand *cis*-1,2-bis(diphenylphosphino)ethylene (vpp) are reported. Single-crystal EPR studies of $[Co(vpp)_2Br]BPh_4$ doped in the corresponding diamagnetic nickel lattice reveals superhyperfine interactions from the in-plane phosphorus nuclei as well as the axial bromine. The EPR results from isotropic, polycrystalline, and single-crystal studies combined with electronic spectral measurements enable us to ascertain the ground state of the unpaired electron. Because of the availability of a sufficient number of bands in the electronic spectra of these complexes, it has been possible to locate all the excited states with reasonable accuracy as borne out by the calculated spin Hamiltonian parameters. Electronic structures of two other related systems—$[Co(dpm)_2X]ClO_4$ and $Co(dpe)_2X_2$ (dpm = (diphenylphosphino)methane, dpe = 1,2-bis(diphenylphosphino)ethane, X = Cl, Br, or I)—are also discussed.

Introduction

Though there has been a spate of publications on the EPR studies of low-spin Co(II) complexes, there is but one example of a CoP_4 system in the literature so far.[1,2] In view of the sustained increase of interest in the transition-metal complexes of group 5B donors[3] we have taken up the study of a few bis(tertiary phosphine) complexes of Co(II). Recently McGarvey[4] has reviewed the EPR studies on low-spin Co(II) complexes and modified the theory of spin Hamiltonian parameters to third order in perturbation which takes care of two important aspects that have been neglected previously: (1) the spin–orbit mixing of the low-lying quartet excited states into the doublet ground state and (2) mixing of d_{z^2} and $d_{x^2-y^2}$ orbitals in low-symmetry complexes through configuration interaction. It was pointed out that, while it is essential to have the **g** and ^{59}Co hyperfine tensors assigned to a particular molecular axis, it is difficult to unequivocally establish the ground state on the basis of these alone. Additional superhyperfine data from in-plane ligand nuclei will be very useful in assigning the ground state and hence the molecular wave function. The five-coordinate complex $[Co(vpp)_2Br]BPh_4$ to be reported here gives this superhyperfine information for all the ligand nuclei. Also, the magnetically dilute polycrystalline spectrum of $[Co(vpp)_2Br]BPh_4$ has been of great help in assigning the principal directions of the magnetic tensors derived from single-crystal studies.

The first part of this paper gives a detailed account of the single-crystal EPR study of $[Co(vpp)_2Br]BPh_4$ substitutionally incorporated in the corresponding diamagnetic nickel lattice, and the latter part attempts a comparative study of the electronic structures of vpp, dpm, and dpe complexes.

Experimental Section

The ligand VPP was prepared according to literature methods.[5] The complexes $[Co(vpp)_2X]BPh_4$ (X = Cl, Br, I) were prepared following the procedure reported for the analogous nickel(II) complexes.[6] Anal. Calcd for $[Co(vpp)_2Cl]BPh_4$: C, 75.66; H, 5.35. Found: C, 74.93; H, 5.52. Calcd for $[Co(vpp)_2Br]BPh_4$: C, 72.97; H. 5.16. Found: C, 72.02; H, 5.32. Calcd for $[Co(vpp)_2I]BPh_4$: C, 70.33; H, 4.97. Found: C, 70.83; H, 5.06. Syntheses of dpm and dpe complexes are found elsewhere.[7,8]

Table I. Spin Hamiltonian Parameters for $Co/[Ni(vpp)_2Br]BPh_4$[a]

property	doped powder	doped cryst
g_{zz}	2.010	2.010
g_{xx}	2.232	2.239
g_{yy}	2.303	2.309
A_{zz}	0.0070,[d] 0.0070,[e] 0.0018[f]	0.0070,[d] 0.0070,[e] 0.0018[f]
A_{xx}	c, d	−0.0014,[d] −0.0016,[e] 0.0016[f]
A_{yy}	c, d	0.0022,[d] −0.0022,[e] 0.0022[f]
g_{av}[b]	2.184	2.186[d]
g_{iso}[b]		2.115
A_{av}		0.0021,[d] 0.0011,[e] 0.0019[f]
A_{iso}[b]		0.0022,[d] not obsd,[e] 0.0018[f]

[a] A values in cm^{-1}. [b] From the solution spectrum. [c] Could not be estimated. [d] ^{59}Co. [e] ^{81}Br. [f] ^{31}P.

EPR and optical spectra of the complexes in solution were measured in dichloromethane solvent. Single crystals used for EPR measurements were grown by slow evaporation of a nitromethane solution of the nickel complex containing 1–2% of the cobalt complex, in nitrogen atmosphere. Solution samples were deoxygenated before EPR measurements. X-Band measurements were made on a Varian E-4 spectrometer with a 100-kHz modulation. Q-Band spectra were recorded on both AEG and Varian E-112 spectrometers with 100-kHz modulation. All field calibrations were made by using DPPH (g = 2.0036) in both X- and Q-band measurements.

Results and Discussion

Doped Polycrystalline Spectrum of $Co/[Ni(vpp)_2Br]BPh_4$. The magnetically dilute polycrystalline spectrum of $[Co(vpp)_2Br]BPh_4$ measured at 77 K in X-band is shown in Figure 1. The Q-band spectrum of the same (Figure 1) clearly reveals the orthohombicity of the **g** tensor. The hyperfine structure on the lowest g component arises from the eight ^{59}Co lines being further split by ^{79}Br, ^{81}Br in such a way that $A(^{59}Co) \simeq A(^{81}Br)$. Of the resulting 11 lines, the three low-field lines in the polycrystalline EPR spectrum overlap with the g_{xx} and g_{yy} components. The quintet structure on these is obviously due to the in-plane ^{31}P nuclei. Due to the poor resolution of the room-temperature Q-band spectrum and the overlap of the hyperfine features from the two low-field g components in the X-band spectrum, no useful hyperfine information could be derived from the low-field spectral group. The principal g values and the z component of the hyperfine tensors for ^{59}Co, ^{79}Br, ^{81}Br, and ^{31}P derived from the spectrum are listed in Table I.

Crystal Structure of $[Ni(vpp)_2Br]BO_4$. The preliminary information available from X-ray analysis[9] indicates that the crystal belongs to the orthorhombic system, space group $P2_12_12$

(1) D. Attanasio, *Chem. Phys. Lett.*, **49**, 547 (1977).
(2) Yuzo Nishida and Sigeo Kida, *J. Inorg. Nucl. Chem.*, **40**, 1331 (1978).
(3) C. A. McAuliffe, Ed., "Transition Metal Complexes of Phosphorus, Arsenic and Antimony Ligands", Macmillan, New York, 1973.
(4) B. R. McGarvey, *Can. J. Chem.*, **53**, 2498 (1975).
(5) A. M. Aguiar and D. Daigle, *J. Am. Chem. Soc.*, **86**, 2299 (1964).
(6) C. A. McAuliffe and Devon W. Meek, *Inorg. Chem.*, **8**, 904 (1969).
(7) K. K. Chow and C. A. McAuliffe, *Inorg. Chim. Acta*, **14**, 121 (1975).
(8) D. W. Horrocks, G. R. van Heeke, and D. W. Hall, *Inorg. Chem.*, **6**, 694 (1967).
(9) J. H. Nöordik, private communication.

0020-1669/81/1320-2533$01.25/0

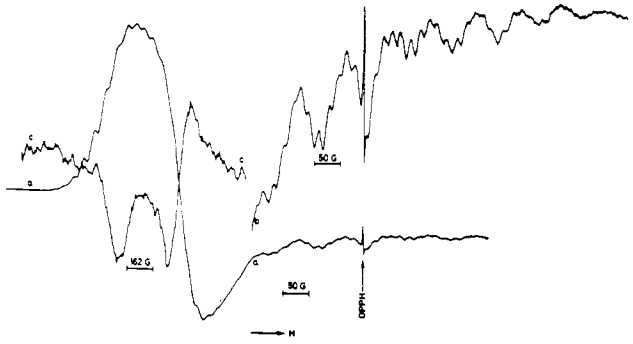

Figure 1. (a) X-Band polycrystalline EPR spectrum of magnetically dilute $[Co(vpp)_2Br]BPh_4$ recorded at 77 K. (b) High-field hyperfine features at increased spectrometer gain. (c) Q-Band spectrum of $Co(II)/[Ni(vpp)_2Br]BPh_4$ at room temperature.

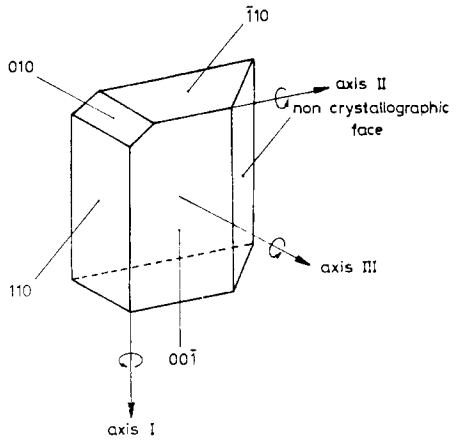

Figure 2. Morphology of the $[Ni(vpp)_2Br]BPh_4$ single crystal and the axes of rotation chosen for EPR measurements.

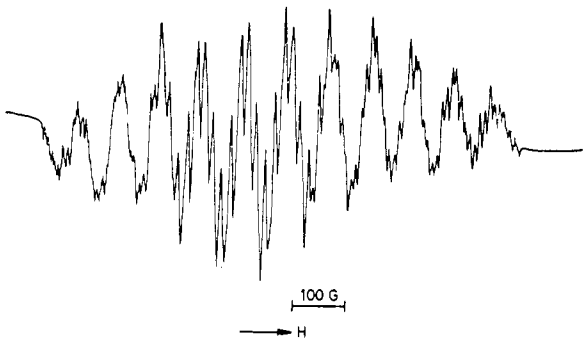

Figure 3. Single-crystal EPR spectrum of $Co(II)/[Ni(vpp)_2Br]BPh_4$ for $H \parallel$ to axis III. This corresponds to the magnetic field being parallel to the Co–Br bond in the molecule.

with eight molecules per unit cell. Also there is evidence for all Ni–Br bonds being parallel to the crystallographic c axis. Morphology of the crystal used for EPR measurements and the axes of rotation chosen for angular variation studies are shown in Figure 2.

Single-Crystal EPR Studies. In the absence of detailed crystal structure information, we have followed the method of Schonland[10] in carrying out the single-crystal EPR study. On studying the crystal plane II–III with axis I as the rotation axis, we obtained a spectrum with the maximum spread as shown in Figure 3. This orientation corresponds to $H \parallel$ to axis III ($H \parallel$ to c axis). This is identical with the high-field g component of the polycrystalline spectrum with exactly

(10) D. S. Schonland, *Proc. Phys. Soc.*, 73, 788 (1959).

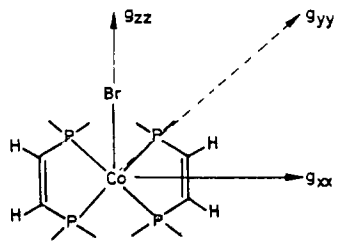

Figure 4. The molecular framework and the principal directions of the magnetic tensors for $[Co(vpp)_2Br]BPh_4$.

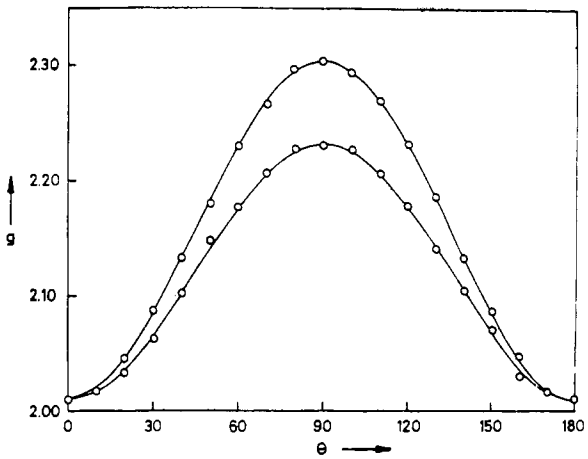

Figure 5. Angular variation of g for rotation about axis I showing the presence of two magnetically distinct sites.

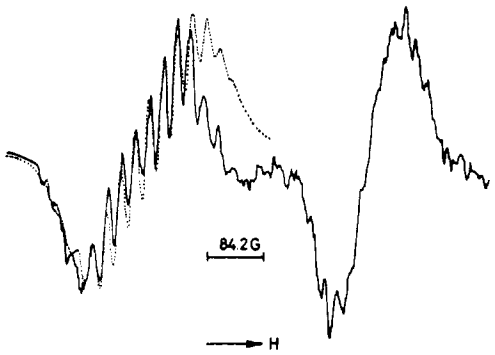

Figure 6. Single-crystal EPR spectrum of $Co(II)/[Ni(vpp)_2Br]BPh_4$ for $H \perp$ to the z axis for rotation about axis I measured at Q-band frequency at room temperature. Computer simulation of the low-field spectral group using the hfc constants of Table I and a line width of 21 G are indicated by the dotted lines.

matching g and A values (see Table I). The Q-band spectrum in this orientation is the same as the X-band spectrum. This spectrum also reveals the bromine isotopic separation which is most prominent in the extreme lines. This orientation is the principal z direction of the **g** and **A** tensors of all the magnetic nuclei and is parallel to the Co–Br bond in the molecule. The molecular framework and the principal directions of the magnetic tensors are shown in Figure 4. The nature of this spectrum with $H \parallel$ to c axis (Co–Br direction) suggests that all the molecules in the unit cell have their z axes parallel, in conformity with the available crystal structure information. However, the angular variation studies in this plane (about axis I) reveal the presence of two magnetically distinct molecules. This is better evidenced by the Q-band measurements where the separation between the two sites is well brought out as compared with the X-band spectra. The angular variation of g for rotation about axis I is presented in Figure 5. The maximum separation between the two sites occurs when the field is perpendicular to the Co–Br direction, i.e., in the CoP_4

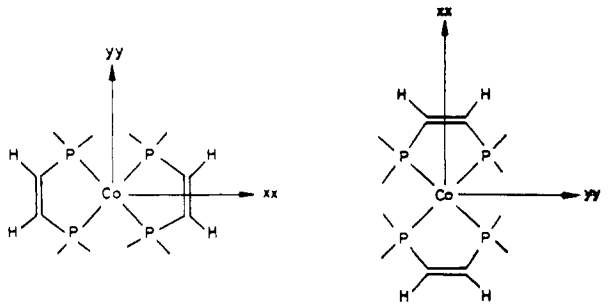

Figure 7. Relative disposition of the two sites in the 001 plane as deduced from the g variations obtained for rotation about axis III.

plane. This spectrum with $H \perp$ to the molecular z axis is shown in Figure 6.

Angular variaton studies about axis II give spectral variations identical with those obtained for rotation about axis I. In other words, here again we get a spectrum characteristic of the orientation where H is $\parallel$ to the Co–Br direction (all sites equivalent (Figure 3)); furthermore, the spectrum obtained at 90° away from this orientation is identical with that in Figure 6. In addition, the g values corresponding to these two sites are in complete agreement with the two low-field g values obtained in the Q-band polycrystalline spectrum (2.239 and 2.309). This definitely proves that the two sites obtained in the latter orientation are the ones corresponding to g_{xx} and g_{yy}. Hence the Co–Br bond is parallel to the crystal c axis, and the equatorial CoP_4 planes are located in the crystallographic ab plane where the g_{xx} and g_{yy} directions of the two inequivalent sites are at 90° to each other as shown in Figure 7.

The aforesaid proposition on the relative orientations of the molecules in the crystal is confirmed by an angular variation study about axis III where the magnetic plane is the 001 plane. Here, the orientations at 0, 90, and 180° give the same spectrum as in Figure 6, in support of the presence of two CoP_4 moieties at 90° to each other in this plane. Further support to this conclusion stems from the fact that at the 45 and 135° orientations the two groups of lines collapse into a single set. The angular variation of g in this plane also conforms to this. The principal magnetic parameters are found in Table I.

Ground State of $[Co(vpp)_2Br]^+$. The **g**- and **A**(^{59}Co)-tensor values are suggestive of a d_{z^2} ground state for the unpaired spin,[11] which is also evidenced by the observation of bromine superhyperfine structure. The isotropic EPR spectrum of $[Co(vpp)_2Br]BPh_4$ in dichloromethane is shown in Figure 8a). The significant difference between the g_{iso} obtained from the spectrum and the g_{av} derived from the measurements in the nickel host lattice cautions against the use of $A_{iso}(^{59}Co)$ which has a value of ~23 G (see below) as the sole factor in deciding the relative signs of the anisotropic parameters. However, theoretical derivation of spin Hamiltonian parameters gives a d-level ordering best fitting the optical spectrum only when A_{xx} is negative and A_{yy} and A_{zz} are positive (vide infra). The phosphorus hyperfine coupling is almost isotropic. The fact that the bromine isotropic coupling is not observed in the solution spectrum can be accounted for by taking $A_{zz}(Br)$ to be positive and A_{xx} and A_{yy} to be negative ($A_{av} \sim 13$ G). Also, in solution the Co–Br bond may be weakened as may be inferred from the rather significant difference between g_{av} and the isotropic g value. However, the isotropic g value does agree quite well with the g_{av} derived from the pure polycrystalline sample of $[Co(vpp)_2Br]BPh_4$ ($g_{11} = 2.231$, $g_{22} = 2.094$, $g_{33} = 2.059$, $g_{av} = 2.129$). This may be interpreted as a result of the difference in the bond distance and hence the covalency

(11) Yuzo Nishida and Sigeo Kida, *Coord. Chem. Rev.*, **27**, 275 (1979).

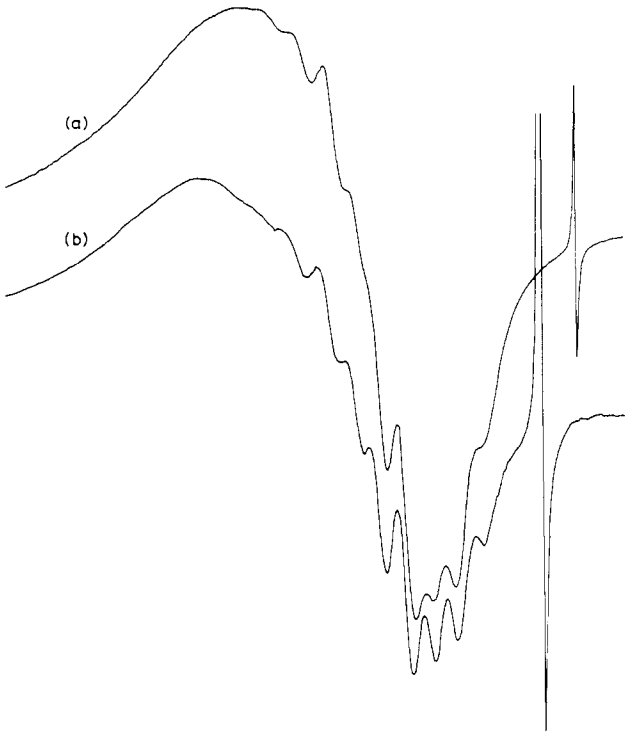

Figure 8. Isotropic EPR spectrum of $[Co(vpp)_2Br]BPh_4$ in dichloromethane solution at RT: a, spectrum immediately on dissolution; b, spectrum after a few days.

Table II. Estimation of the Total Spin Density on the Ligand Nuclei of $[Co(vpp)_2Br]^+$

	^{81}Br		^{31}P	
	A, G	ρ, %	A, G	ρ, %
A_{iso}, ρ_{ns}	13	0.15	18	0.5
A_{dip}(major), ρ_{np}	58	10.3	dipolar density nearly zero	
A_{dip}(minor), ρ_{np}	4	0.7		

$\rho_{Br} = 11.15\%$; $\rho_{4p} = 2\%$

total $\rho_{4p,Br} = 13.15\%$

of the Co–Br bond in the pure cobalt complex lattice from those in the host nickel lattice. A simple estimation of the total unpaired density on the ligand nuclei based on the superhyperfine coupling constants is given in Table II. The isotropic and dipolar coupling constants corresponding to one unpaired electron in the respective orbitals were taken from an earlier compilation.[12]

Expressions of **g** and ^{59}Co hf tensor components for C_{2v} symmetry (eq 19–24 of ref 4) involve as many as 12 unknowns whereas only six experimental values are available. Obtaining a unique solution depends on a judicious choice of some of these parameters. Of course, the most meaningful solution would be the one which stands in good correlation with the optical spectrum of the compound. The electronic absorption spectrum of $[Co(vpp)_2Br]BPh_4$ shows six bands. The ground state, the doublet excited states that account for the seven spin-allowed transitions, and their associated quartet states for low-spin Co(II) may be represented as three-hole configurations. The various three-hole configurations, the electron repulsion energies corresponding to these and the calculated transition energies along with the observed bands for the $[Co(vpp)_2X]^+$ complexes (X = Cl, Br, I) are tabulated in

(12) P. W. Atkins and M. C. R. Symons, "The Structure of Inorganic Radicals", Elsevier, Amsterdam, 1967.
(13) J. K. Stalick and D. W. Meek, *J. Chem. Soc., Chem. Commun.*, 630 (1972).

Table III. Calculated and Experimental Transition Energies in $[Co(vpp)_2X]BPh_4$

electronic transition and hole confign ground state	$[Co(vpp)_2Cl]BPh_4$			$[Co(vpp)_2Br]BPh_4$			$[Co(vpp)_2I]BPh_4$			interelectronic interaction parameters[d]
	$\Sigma\epsilon_k$,[a] cm^{-1}	transition energy, cm^{-1} calcd[b]	obsd[c]	$\Sigma\epsilon_k$,[a] cm^{-1}	transition energy, cm^{-1} calcd[b]	obsd[c]	$\Sigma\epsilon_k$,[a] cm^{-1}	transition energy, cm^{-1} calcd[b]	obsd[c]	
$\bar{xy}\ x\bar{y}\ z^2\ (^2A_1)$	13 450	...	...	13 100	...	...	12 470	...	...	$3F_0 - 8F_2 + 33F_4$
$z^2 \rightarrow xy^e$	26 900	13 450	13 450	26 200	13 100	13 100	24 940	12 470	12 470	$3F_0 - 8F_2 + 33F_4$
$\bar{z^2}\ \bar{z^2}\ x\bar{y}\ (^2A_2)$										
$xz \rightarrow z^2$	17 620	7 170	7 170	17 170	7 070	7 070	16 510	6 340	6 840	$3F_0 - 3F_2 + 8F_4$
$\bar{xz}\ \bar{xy}\ x\bar{y}\ (^2B_1)$										
$yz \rightarrow z^2$	21 460	11 010	11 010	20 750	11 100	11 100	20 320	10 650	10 650	$3F_0 - 3F_2 + 8F_4$
$\bar{yz}\ \bar{xy}\ x\bar{y}\ (^2B_2)$										
$x^2 - y^2 \rightarrow z^2$	24 920	23 470	23 470	23 720	22 620	22 620	25 950	24 680	24 680	$3F_0 + 12F_2 - 76F_4$
$(x^2 - y^2)^-\ \bar{xy}x\bar{y}\ (^2A_1)$										
$xz \rightarrow xy$										
$^4B_2$	31 070	2 620	...		2 170	...	28 980	2 510	...	$3F_0 - 12F_2 - 87F_4$
$^2B_2(1)$		15 670	14 850	30 270	15 220	14 615		14 690	14 360	$3F_0 - 6F_2 - 12F_4$
$^2B_2(2)$		18 070			17 620	...		16 930	...	$3F_0 - 2F_2 - 32F_4$
$yz \rightarrow xy$										
$^4B_1$	34 910	6 460	...	34 300	6 200	...		6 320	...	$3F_0 - 12F_2 - 87F_4$
$^2B_1(1)$		19 510	19 810		19 250	19 960	32 700	18 500	19 020	$3F_0 - 6F_2 - 12F_4$
$^2B_2(2)$		21 910	...		21 650	...		20 740	21 620	$3F_0 - 2F_2 - 32F_4$
$x^2 - y^2 \rightarrow xy^e$										
$^4A_2$	38 370	9 920	...	36 820	8 720	...	38 420	11 950	...	$3F_0 - 12F_2 - 87F_4$
$^2A_2(1)$		22 970	...		21 770	...		24 130	...	$3F_0 - 6F_2 - 12F_4$
$^2A_2(2)$		25 370	...		24 170	...		26 370	...	$3F_0 - 2F_2 - 32F_4$

[a] Sum of single electron vacancy energies. [b] Sum of single electron vacancy energy and electron repulsion energy minus the ground state energy. [c] Observed. [d] Condon and Shortley parameters: $F_2 = 980\ cm^{-1}$ and $F_4 = 84\ cm^{-1}$ (70% of the free ion values) for the iodo complex; $F_2 = 1050\ cm^{-1}$ and $F_4 = 90\ cm^{-1}$ (75% of the free ion values) for the chloro and bromo complexes. [e] Transitions not allowed under C_{2v} symmetry; but they may be vibronically allowed or under a still lower symmetry such as C_2. Within the accuracy of these calculations these bands (···) (other than the forbidden ones) lie easily within the observed bands.

Table IV. Electronic Spectral Data[a] of $[Co(vpp)_2X]BPh_4$ Obtained by Gaussian Analysis

$[Co(vpp)_2Cl]BPh_4$		$[Co(vpp)_2Br]BPh_4$		$[Co(vpp)_2I]BPh_4$	
mull	solution	mull	solution	mull	solution
6 900	7 170 (790)	6 680	7070 (719)	6 900	6 840 (1330)
11 260	11 010 (820)	11 100	11 100 (824)	10 550	10 650 (2328)
13 800	13 450 (5267)	12 900	13 100 (3603)	13 100	12 470 (5821)
15 400	14 850 (4918)	14 300	14 615 (4118)	14 800	14 360 (6653)
20 000	19 810 (5269)		19 960 (4324)		19 020 (6653)
23 250	23 470 (17 388)		22 620 (14 412)	22 100	21 620 (20 360)
					24 680 (17 293)

[a] Energies in cm^{-1}. The numbers in parentheses are extinction coefficients ($L\ mol^{-1}\ cm^{-1}$).

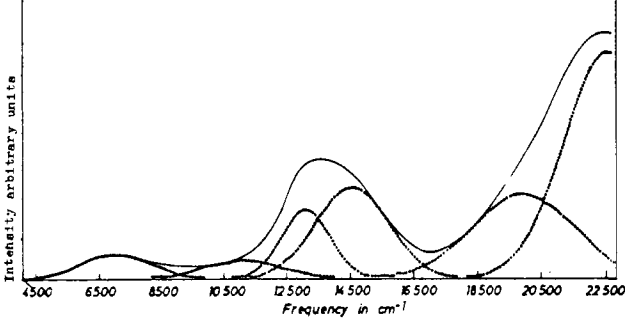

Figure 9. The electronic absorption spectrum of $[Co(vpp)_2Br]BPh_4$ in dichloromethane solution at room temperature. Dotted lines represent the individual bands obtained from Gaussian analysis.

Table III. The spectrum of $[Co(vpp)_2Br]BPh_4$ in dichloromethane solution and the individual absorption bands obtained through Gaussian analysis of the experimental spectrum with use of the program BANDFIT are shown in Figure 9. Mull spectra are shown in Figure 10. Band positions as obtained from solution and Nujol mull measurements for these compounds are listed in Table IV.

The coefficients c_1–c_6 and c_3', c_4', and c_5' obtained by using the excitation energies as assigned in Table III for $[Co(vpp)_2Br]BPh_4$ are found in Table V along with the calculated **g**- and **A**-tensor values. These coefficients represent the ratio of the spin–orbit coupling coefficient of the Co^{2+} ion altered to account for covalency and the transition energy. The importance of the contributions from the quartet states and the d_{z^2} and $d_{x^2-y^2}$ mixing is directly evidenced by the poor agree-

Table V. Theoretical Evaluation of Spin Hamiltonian Parameters[a]

	g and ^{59}Co hyperfine tensor values			
coefficients[b]	exptl	contributions from doublet excited states only	including quartet states	allowing for $d_{x^2-y^2}$ admixture[i]
$c_1 = 0.056$	2.010[c]	1.9949[c]	2.0283[c]	2.0256[c]
$c_2 = 0.036$	2.239[d]	2.2025[d]	2.2053[d]	2.2347[d]
$c_3 = 0.0645$	2.309[e]	2.3319[e]	2.3545[e]	2.3024[e]
$c_4 = 0.1843$	0.070[f]	0.0089[f]	0.00784[f]	0.00750[f]
$c_5 = 0$				
$c_6 = 0.0305$	−0.0014[g]	−0.0014[g]	−0.00124[g]	−0.00265[g]
$c_3' = 0.021$	0.0023[h]	0.00056[h]	0.00144[h]	0.00269[h]
$c_4' = 0.0263$				
$c_5' = 0$				

[a] A values in cm^{-1}. [b] Derived from the band assignments given in Table III. The A-tensor values were calculated with $\kappa = -0.0005\ cm^{-1}$ and $P = 0.0175\ cm^{-1}$. [c] g_{zz}. [d] g_{xx}. [e] g_{yy}. [f] A_{zz}. [g] A_{xx}. [h] A_{yy}. [i] $a = 0.993$.

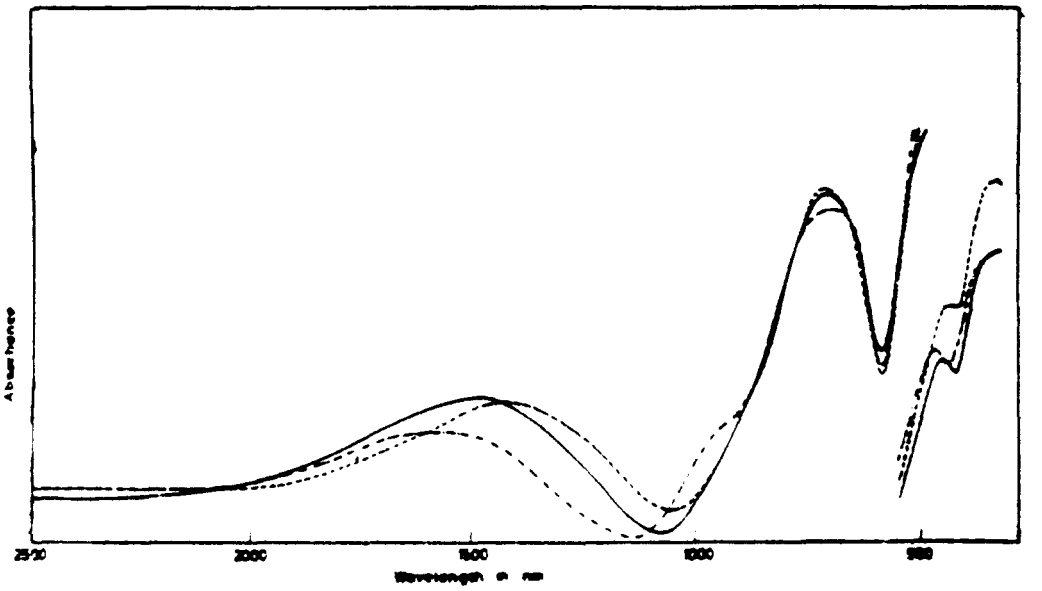

Figure 10. The mull spectra of the $[Co(vpp)_2X]BPh_4$ complexes: —, X = Br; ···, X = I; - - -, X = Cl.

ment obtained otherwise with only the contribution of the doublet excited states taken into account. In the calculation of ^{59}Co hyperfine tensor values two other parameters κ and P need to be known. While it is customary to reduce the free-ion value of P (254×10^{-4} cm^{-1} for Co^{2+}) to accommodate covalency, κ fluctuates over a wide range of values for different types of complexes.[4] We have calculated the A-tensor values for P values reduced to different amounts of percentage ionicity and for each calculation κ was varied to obtain the best fit with the experimental values. The best agreement was obtained for $P = 0.0175$ cm^{-1} and $\kappa = 0.0005$ cm^{-1}. The discrepancy still persisting can be explained on the basis of the possible errors involved in assuming the same Fermi contact term for the unpaired electron in the orbitals $(a(d_{z^2}) + b(d_{x^2-y^2}))$ and $(a(d_{x^2-y^2}) - b(d_{z^2}))$ as for the d_{xy}, d_{xz}, or d_{yz} orbitals whereas only the former two orbitals can mix with the 4s orbital in C_{2v} or lower symmetries.

In summary, the most noteworthy results are as follows. (1) The unpaired electron in the molecule has a d_{z^2} ground state with a small admixture of $d_{x^2-y^2}$ orbital. The one-electron d-level ordering deduced from EPR and electronic spectra data is $d_{xy} > d_{z^2} > d_{xz} > d_{yz} > d_{x^2-y^2}$. (2) The Co(II)–P bond is more or less purely of a σ nature. (3) The observed bromine hyperfine coupling is more a reflection of the covalency in the host lattice than in the guest molecule itself. (4) Quadrupole effects of ^{59}Co are very small in this complex. (5) The quartet states definitely contribute to the g and A tensors.

Comparative Study of the vpp, dpe, and dpm Complexes of Co(II)

The optical and magnetic properties of the vpp complexes are now compared with those of the Co(II) complexes

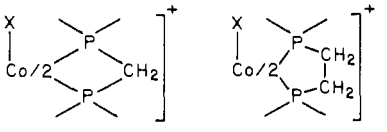

dpm dpe

where X = Cl, Br, or I. Pure powder g values and solution EPR data for the series are listed in Table VI.

Isotropic EPR Spectra. The isotropic EPR spectrum of $[Co(dpm)_2Cl]ClO_4$ measured in dichloromethane at room temperature is shown in Figure 11. Computer simulation of the same gives a fitting with only cobalt and phosphorus hyperfine coupling constants included and shows no isotropic coupling from the axial chlorine. The intensity variation of the lines could not be accounted for by a linear m_I dependence of line width since the lines at both extremes of the spectrum are broadened when compared to the "middle lines". Hence we have included a term quadratic in m_I also in the line width parameter. Accordingly the three parameters used are 21.3, 3, and 0.5 G, respectively. The bromo and iodo complexes also give isotropic spectra which closely resemble the spectrum of the chloro complex in the hyperfine features and the total

Table VI. Pure Powder g Values and Solution EPR Data[a]

compd	g_1	g_2	g_3	g_{av}	g_{iso}	A_{iso}, G ^{59}Co	A_{iso}, G ^{31}P
$[Co(dpm)_2Cl]ClO_4$	2.058	2.219	2.106	2.127	2.096		
$[Co(dpm)_2Br]ClO_4$	2.069	2.261	2.104	2.145	2.115		
$[Co(dpm)_2I]ClO_4$	2.069	2.282	2.143	2.165	2.147		
$[Co(vpp)_2Cl]BPh_4$	2.089				2.089	23	20
$[Co(vpp)_2Br]BPh_4$	2.059	2.232	2.097	2.129	2.115		
$[Co(vpp)_2I]BPh_4$	2.046	2.286	2.146	2.148	2.126		
$[Co(vpp)_2](ClO_4)_2$	2.096			2.096	2.097		
$[Co(dpe)_2I_2]$[b]	1.998	2.455	2.740	2.397	2.205	49	20

[a] g values correct to ±0.005. [b] Doped powder g values from ref 1.

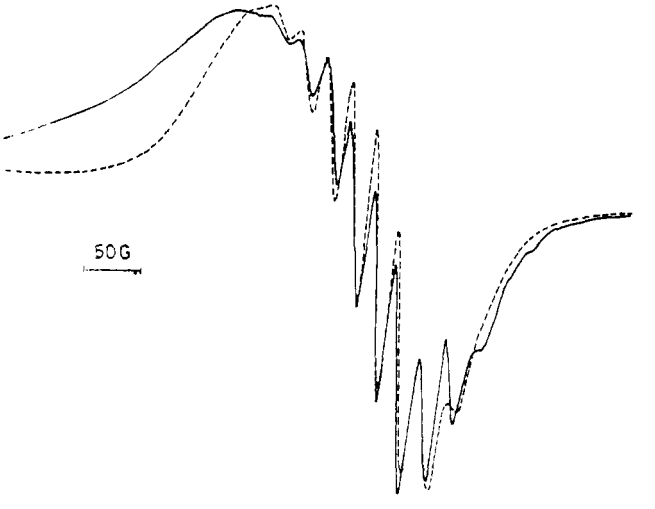

Figure 11. (a) Isotropic EPR spectrum of $[Co(dpm)_2Cl]ClO_4$ in dichloromethane solution at room temperature. (b) Computer simulation of part a.

Table VII. Evaluation of g-Tensor Values for $Co(dpe)_2I_2$ for the z^2 Ground State ($xy > z^2 > yz > x^2 - y^2$)

electronic transition	$\Sigma\epsilon_k$,[a] cm^{-1}	transition energy, cm^{-1} calcd[b]	transition energy, cm^{-1} obsd[c]	excited-state coefficients ($\lambda = 420\ cm^{-1}$)	calcd g values $a = 1$	calcd g values $a = 0.99$ b positive	calcd g values $a = 0.99$ b negative
$z^2 \rightarrow xy$	29 800	14 900	14 900	$c_1 = 0.0866$	2.0274[d]	2.0247[d]	2.0212[d]
$xz \rightarrow z^2$	16 840	4 850	4 850	$c_2 = 0.0630$	2.3470[e]	2.4109[e]	2.2750[e]
$yz \rightarrow z^2$	18 660	6 670	6 670	$c_3 = 0.1032$	2.5112[f]	2.4122[f]	2.599[f]
$x^2 - y^2 \rightarrow z^2$	38 200	22 200	22 200	$c_4 = 0.1866$			
$xz \rightarrow xy$				$c_5 = 0.0386$			
$^4B_2$	31 740	2 250	...	$c_6 = 0.0282$			
$^2B_2(1)$		14 840	14 900	$c_3' = 0.0252$			
$^2B_2(2)$		17 270	...	$c_4' = 0.0283$			
$yz \rightarrow xy$							
$^4B_1$	33 560	4 070	...	$c_5' = 0.0178$			
$^2B_2(1)$		16 660	...				
$^2B_2(2)$		19 100	...				
$x^2 - y^2 \rightarrow xy$							
$^4B_2$	40 360	10 870	...				
$^2A_2(1)$		23 560	...				
$^2A_2(2)$		25 900	...				

[a] Sum of single electron vacancy energies with assumption of the value of 14 900 cm^{-1} for the ground state. [b] Calculated. Electron repulsion integrals as found in Table III ($F_2 = 1020\ cm^{-1}$ and $F_4 = 87.6\ cm^{-1}$). [c] Observed. [d] g_{zz}. [e] g_{xx}. [f] g_{yy}.

spread of the spectrum. There is considerable broadening of the lines in cases of the bulkier halogens being the axially coordinating ligands. The isotropic g values in all cases correspond to the g_{av} obtained from pure polycrystalline spectra (see Table VI).

The isotropic EPR spectra of vpp complexes are quite similar to those of the dpm complexes with almost identical hyperfine coupling constants for ^{59}Co and ^{31}P (compare Figures 8 and 11). The spectra of fresh solutions of vpp complexes with the axial ligands chlorine, bromine, and iodine are different from those measured after a few days. Though the spectrum of the freshly prepared solution of the chloro complex exhibits well-resolved lines, the spectra of the bromo and iodo complexes are broadened. After being kept for a few days, all the complexes give identical and well-resolved spectra having the same g value (Figure 8b). The different g values obtained by using fresh and aged solutions indicate the loss of axial ligands in all cases, leaving only the $[Co(vpp)_2]^{2+}$ species. However, the change was too slow and incomplete to derive any quantitative information from conductance measurements that were done with use of nitromethane solution. Two observations which support the stability of the five-coordinate species in solution (over a few day period) are that (1) the g_{iso} agrees with the g_{av} obtained from pure polycrystalline sample and (2) the frozen-glass spectrum taken in dichloromethane solvent agrees well with that of pure polycrystalline material.

The isotropic spectra of the $Co(dpe)_2X_2$ complexes are completely different in nature from that of the dpm and vpp complexes discussed above. Also the spectra of $[Co(dpe)_2Cl]SnCl_3$, $Co(dpe)_2Cl_2$, and $Co(dpe)_2(BPh_4)_2$ have the same hyperfine pattern, once again showing the noncontributing nature of the axial ligands. The isotropic spectrum of $Co(dpe)_2(BPh_4)_2$ and the computer simulation of the same are shown in Figure 12. Here the hyperfine coupling constant of ^{59}Co is ~49 G whereas in the case of the earlier discussed dpm and vpp complexes it is only ~23 G. This may be attributed to stereochemical reasons. Because of the "ring strain" in the case of the dpm ligand and the ethylenic planarity of the vpp ligand, in these two cases the four phosphorus nuclei can be expected to be in a plane; the dpe ligand on the other hand exhibits the full conformational nonrigidity of ethane as can be seen from the X-ray crystal structure of $[Co(dpe)_2Cl]SnCl_3$.[13]

Further understanding of the electronic structures of these complexes is possible only through a detailed analysis of their

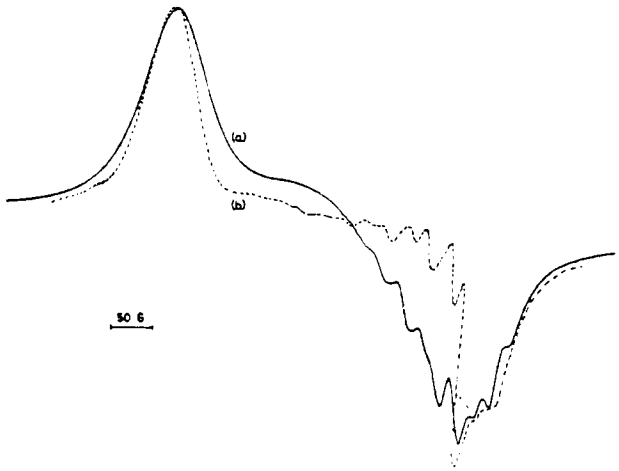

Figure 12. (a) Isotropic EPR spectrum of $[Co(dpe)_2](BPh_4)_2$ in dichloromethane solution at room temperature. (b) Computer simulation of part a, using isotropic coupling constants of 49 G for ^{59}Co and 19 G for ^{31}P. Line width parameters used are 22, 3.2, and 0.8 G.

optical spectra and the interpretation of spin Hamiltonian parameters. Though Horrocks et al.[8] have assigned the electronic spectra of the dpe complexes on the basis of the $x^2 - y^2$ ground state for the unpaired electron, this needs to be reconsidered on the basis of the anisotropic powder measurements reported subsequently.[1] The fitting of the spin Hamiltonian parameters as carried out earlier[1,2] is again at variance with our observed hyperfine coupling constant of 49 G for ^{59}Co. The fitting parameters obtained have no meaning unless the relative signs of the hyperfine tensor values are taken into account and a good correlation to the optical spectrum is to be arrived at in the process of doing so. We have therefore recalculated the spin Hamiltonian parameters for one of the complexes $Co(dpe)_2I_2$ of ref 1, using eq 19–24 of ref 4.

In accordance with the procedure adopted for the vpp complexes we have calculated all the excited-state coefficients from an assignment of the various absorption bands reported for the complex.[8] The distinguishing feature of the electronic spectra of the dpe complexes as compared to those of dpm and vpp complexes is the presence of an additional low-energy band ~5000 cm^{-1} (other than the one at ~7000 cm^{-1} which is common to dpm, vpp, and dpe complexes). Calculatons based on a pure z^2 ground state for the d-level ordering $xy > z^2 >$

Table VIII. Evaluation of g-Tensor Values for $Co(dpe)_2I_2$ for the z^2 Ground State ($xy > z^2 > x^2 - y^2 > xz > yz$)

electronic transition	$\Sigma\epsilon_k$,[a] cm^{-1}	transition energy, cm^{-1} calcd[b]	transition energy, cm^{-1} obsd[c]	excited-state coefficients ($\lambda = 420\ cm^{-1}$)	calcd g values $a = 1$	calcd g values $a = 0.99$ b positive	calcd g values $a = 0.99$ b negative
$z^2 \rightarrow xy$	29 800	14 900	14 900	$c_1 = 0.0866$	2.0240[e]	2.0246[e]	2.02132[e]
$xz \rightarrow z^2$	16 840	4 850	4 850	$c_2 = 0.06297$	2.4589[f]	2.5712[f]	2.4200[f]
$yz \rightarrow z^2$	18 660	6 670	6 670	$c_3 = 0.10324$	2.5879[g]	2.5261[g]	2.7402[g]
$x^2 - y^2 \rightarrow z^2$	16 140	12 900	12 900	$c_4 = 0.18683$			
$xz \rightarrow xy$				$c_5 = 0.26786$			
$^4B_2$	31 740	2 250	...	$c_6 = 0.0282$			
$^2B_2(1)$		14 940	14 900	$c_3' = 0.02506$			
$^2B_2(2)$		17 265	...	$c_4' = 0.02812$			
$yz \rightarrow xy$							
$^4B_1$	33 560	4 070	...	$c_5' = 0.02946$			
$^2B_1(1)$		16 760[d]	...				
$^2B_2(2)$		19 090[d]	22 200				
$x^2 - y^2 \rightarrow xy$							
$^4A_2$	31 060	1 570	...				
$^2A_2(1)$		14 260	14 900				
$^2A_2(2)$		16 590					

[a] Sum of single electron vacancy energies with assumption of a value of 14 900 cm^{-1} for the ground state. [b] Calculated with use of electron repulsion energies as given in Table III ($F_2 = 1020\ cm^{-1}$ and $F_4 = 87.6\ cm^{-1}$). [c] Observed. [d] These two states could have mixed by configuration interaction. The resulting energies could have corresponded to the experimental bands at 14 900 and 22 200 cm^{-1}. [e] g_{zz}. [f] g_{xx}. [g] g_{yy}.

$xz > yz > x^2 - y^2$ as in the case of the vpp complexes discussed above could not sufficiently scale up the g-tensor values as can be seen from Table VII (experimental values: $g_{zz} = 2.001$, $g_{xx} = 2.455$, and $g_{yy} = 2.740$ (adopting the same coordinate system as for the vpp complex)). In order to see the effect of the z^2, $x^2 - y^2$ admixture on the calculated g values, we have modified the electron repulsion energies for the ground and excited states. However, this did not improve the situation for both positive and negative values of b. According to the assignments given by Horrocks et al.[8] the transition at 4850 cm^{-1} corresponds to the quartet excitation from $z^2 \rightarrow xy$ which is unlikely because the band at 4850 cm^{-1} has appreciable intensity—similar to that of the ~7000-cm^{-1} band. Alternate considerations based on $x^2 - y^2$ ground state do not give a good fitting of the observed bands or agreeable g values.

The g_{zz} value of 2.00 for these complexes undoubtedly suggests a z^2 ground state. The xy orbital being the highest energy orbital, the only other possibility is a relative destabilization of the $x^2 - y^2$ orbital with respect to the xy and yz orbitals. Assuming $xy > z^2 > x^2 - y^2 > xz > yz$, we have got the best agreement with experimental values and have assigned all the observed bands in a unique fashion (see Table VIII). It must be noted that there is the same vast difference in the d-level splittings of the vpp and dpe complexes as in their spin Hamiltonian parameters. In this calculatoin use has been made of the same electron repulsion energies as for a pure z^2 ground state as we have found that the relative sensitivities of the electron repulsion energies and the g-tensor values to the admixture coefficient b are not compatible.

Choice of κ and P values so as to arrive at the experimental values of the A tensor with the relative signs matching the isotropic value of ~49 G should be the next step (experimental values (cm^{-1}): $A_{zz} = 0.0119$, $A_{xx} = 0.0107$, and $A_{yy} = 0.0141$). The obvious choice of signs would be to take A_{xx} as negative and the other two positive or vice versa. Assuming the dipolar term P to be 0.02 cm^{-1}, κ was varied over a wide range to meet this requirement. However, no success was achieved, even when P was lowered to 0.01 cm^{-1} (50% free-ion value). So we have resorted to the indirect method of evaluating the hyperfine tensor values using a κ_{av} deduced from the experimental values. Accordingly, the three values obtained for $P = 0.02\ cm^{-1}$ and the sign of A_{xx} negative are $\kappa_{zz} = 0.004\,417$, $\kappa_{xx} = -0.014\,78$, and $\kappa_{yy} = 0.009\,81$, leading to $\kappa_{av} = -0.000\,182\,6$. It is interesting to see that the principal values on using the κ_{av} obtained thus give an average A value equal to 0.0051 cm^{-1} which is in good agreement with the observed isotropic coupling constant of 49 G (calculated A values cm^{-1}) $A_{zz} = 0.0073$, $A_{xx} = 0.0039$ and $A_{yy} = 0.0041$ (all having positive sign)). The observed isotropic coupling constant is an artifact of the inequivalence of the Fermi term associated with the orbitals which are allowed or not allowed to mix with the 4s orbital. The large differences in the isotropic contribution to each hyperfine tensor component is also indicative of considerable admixture of the 4s orbital into the ground state.

In the absence of anisotropic data on dpm complexes it is difficult to derive any further information on the electronic structure of these. But they resemble the vpp complexes very closely in their electronic spectra and isotropic EPR spectra so that it could be predicted that they have the same d-level ordering and electronic structure. However, the one common factor in all these complexes is the contribution of the quartet states to the spin Hamiltonian parameters.

Acknowledgment. We thank Mr. Dinesh Nettar of this laboratory for providing the program ESRSIM written by him which was used for the simulation of the isotropic spectra. C.N.S. is grateful to NCERT, New Delhi, for a fellowship during the period of this work.

Registry No. $[Co(vpp)_2Cl]BPh_4$, 77320-89-9; $[Co(vpp)_2Br]BPh_4$, 33789-73-0; $[Co(vpp)_2I]BPh_4$, 77320-91-3; $[Ni(vpp)_2Br]BPh_4$, 23108-67-0; $[Co(dpm)_2Cl]ClO_4$, 56689-59-9; $[Co(dpm)_2Br]ClO_4$, 56689-61-3; $[Co(dpm)_2I]ClO_4$, 56689-63-5; $[Co(vpp)_2](ClO_4)_2$, 16592-86-2; $Co(dpe)_2I_2$, 64421-76-7; $[Co(dpe)_2](BPh_4)_2$, 64312-44-3.